JOURNAL OF PHYSICAL ORGANIC CHEMISTRY
J. Phys. Org. Chem. 2004; **17:** 257–265
Published online in Wiley InterScience (www.interscience.wiley.com). DOI: 10.1002/poc.724

NMR spectroscopic and molecular modelling study of the solution structure and the complexational behavior of maleonitrile tetrathia crown ethers with silver(I)

Anja Holzberger, Hans-Jürgen Holdt and Erich Kleinpeter*

Universität Potsdam, Chemisches Institut, P.O. Box 69 15 53, D-14415 Potsdam, Germany

Received 16 July 2003; revised 17 September 2003; accepted 22 September 2003

ABSTRACT: The flexibility and complex formation of two maleonitrile tetrathia crown ethers were studied in solution using ^{1}H and ^{13}C NMR spectroscopy and molecular modelling. Both the stoichiometry and the stability of the complexes that these crown ethers form with Ag(I) were determined by NMR titration measurements. Spin–lattice relaxation time measurements provided information concerning the donor atoms involved in complex formation and also the intramolecular mobility of the free and complexed ligands. Molecular modelling was also used to gain further insight into the conformational space of the free ligands and their silver(I) complexes. Copyright © 2004 John Wiley & Sons, Ltd.

KEYWORDS: maleonitrile tetrathia crown ethers; NMR spectroscopy; molecular modelling; silver(I) complexes

INTRODUCTION

In the ongoing search for metal-selective extractors and chemical sensors for analytical applications, new sulfur-containing macrocyclic ligands are being synthesized.[1] Two new tetrathia crown ethers that have been synthesized recently are mn–12–S_4 and mn–13–S_4 (see Fig. 1). They are derived from the tetrathia crown ethers [12]aneS_4 and [13]aneS_4 but contain a rigid maleonitrile unit instead of the usual flexible ethylene bridge present in parent structures. In comparison with the saturated tetrathia crown ethers where all of the four donor atoms were found to prefer exocyclic positions,[2,3] in these new maleonitrile tetrathia crown ethers it is expected that the rigid maleonitrile moiety will force two of the four donor atoms of the macrocyclic ring into endocyclic dispositions. An increased ability of these thia crown ethers to form endocyclic complexes with transition metal ions could be expected; this will be studied in solution.

Previously, maleonitrile dithia crown ethers with mixed donor sets of sulfur and oxygen heteroatoms and different ring sizes have been studied. These oxathia crown ethers are very flexible and variable-temperature NMR experiments and relaxation time measurements indicated that intramolecular mobility increases rapidly with ring size. From the analysis of the vicinal H,H coupling constants and the application of molecular dynamics (MD) simulations, both the O—C—C—O and O—C—C—S structural fragments were shown to prefer *gauche* or *anti* conformations whereas C—C—O—C was shown to prefer an *anti* conformation.[4,5] Owing to the mixed set of sulfur and oxygen donors, the maleonitrile crown ethers are able to force A, AB and B class metal cations into their coordination spheres. Ag(I), Bi(III), Sb(III), Pd(II) and Pd(II) were all found to coordinate to these mixed S_2O_n ($n = 2$–5) coronands.[6] Whereas Ag(I) interacts with both the sulfur and the oxygen atoms of these crowns, by comparison, Bi(III) and Sb(III) are coordinated via the oxygen atoms only whereas $PtCl_2$ and $PdCl_2$ are coordinated via the sulfur atoms.[4] The stability of these complexes was found to decrease in the following order: mn–12–S_2O_2 > mn–18–S_2O_4 > mn–15–S_2O_3. Furthermore, the sulfur atoms were found to adopt different configurations depending on the ring size.[7,8]

We have continued these investigations on maleonitrile crown ethers by examining structures where the heteroatoms in the crown ether moiety are only sulfur. It is the objective of this paper to report on the conformation and intramolecular flexibility of the maleonitrile tetrathia crown ethers mn–12–S_4 and mn–13–S_4 and the complexes that they form with Ag(I) ions.

EXPERIMENTAL

NMR spectroscopy. ^{1}H and ^{13}C NMR spectra were recorded on Bruker Avance 500 or Avance 300 NMR spectrometers using 5 mm probes operating at 500 or

**Correspondence to:* E. Kleinpeter, Universität Potsdam, Chemisches Institut, P.O. Box 69 15 53, D-14415 Potsdam, Germany.
E-mail: kp@chem.uni-potsdam.de

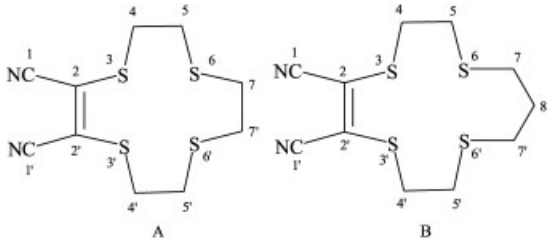

Figure 1. Structural formulae of the compounds studied: (A) mn–12–S_4; (B) mn–13–S_4

300 MHz for ^{1}H, respectively, and 125 or 75 MHz for ^{13}C, respectively. For the structural assignments of the compounds and for low-temperature NMR measurements, the samples were dissolved in CD_2Cl_2; for the titration experiments and the measurement of spin-lattice relaxation times (T_1), CD_3CN was employed.

For the calculation of the activation barrier ($\Delta G^{\neq}$), first the rate constants at the coalescence temperature were calculated using the Gutowski–Holm method.[9] This rate constant was inserted into the Eyring equation to obtain the $\Delta G^{\neq}$ value.[10]

Titration experiments were conducted using the continuous variation method[11] as follows. Solutions of 3.3×10^{-4} M $AgBF_4$, mn–12–S_4 and mn–13–S_4 in CD_3CN were prepared and the ^{1}H NMR spectra of the pure ligands recorded. Following this, the concentration of the ligand was decreased successively while the concentration of the metal ion was increased as it was necessary that the sum of concentrations of metal ion and of the ligand remained constant during the steps of the titration.

Sample preparation for the T_1 measurements included the removal of paramagnetic oxygen from the solution, effected by ultrasonification for 30 min under argon. T_1 values were measured using the inversion–recovery pulse sequence with 16 different delay times. T_1 values were then calculated using the standard Bruker software. For COSY, HMQC and HMBC experiments the standard Bruker pulse sequences were also utilized.

The digital resolution was adjusted 1600 data points for ^{1}H NMR and 160 data points for ^{13}C NMR spectra. The temperature for the dynamic NMR measurements could be adjusted with an error of ± 1 K and the determination of the T_1 relaxation times can be performed with an uncertainty of 5 ms.

Molecular modelling. MD simulations and the random search of the free ligands were performed using the program SYBYL[12] with the Tripos force field.[13] MD runs were executed up to 10 ns at 500 K with time steps of 1 fs. A temperature of 500 K was used to overcome all torsional barriers within the ring; however, it does not represent a physical state. Additionally, a dielectric constant of 8.93 was used to simulate the effects of the solvent (CD_2Cl_2) to the dynamic behaviour of the compounds. The atomic coordinates of the molecules were saved every 500 fs, yielding a final set of 20 000 conformations representing the entire conformational space of the compounds.

Random search simulations consisted of 100 000 cycles. All torsional angles within the ring were allowed to vary randomly and no constraints were applied. After each cycle, the optimized conformation was stored if the heat of formation was within 20 kJ mol^{-1} of the lowest calculated heat of formation. The simulation was terminated prematurely if all so-obtained conformations had been counted at least five times. This ensured that the global minimum was found with a confidence in excess of 95%.[14]

The geometry optimizations of the silver ion complexes were performed using the semiempirical method ZINDO.[15] Calculations were performed on IRIS-INDIGO XS24, SGI O2 workstations or PCs with Pentium 1 processors.

RESULTS AND DISCUSSION

NMR spectroscopy

Signal assignment began with the two equivalent CH_2 groups linked closest to the maleonitrile unit. Both the ^{1}H and the ^{13}C resonances of these CH_2 groups are shifted to lower field in comparison with the other CH_2 signals; the protons of these CH_2 groups also possess $^3J_{C,H}$ couplings to vinyl carbons of the maleonitrile unit. The other signals were assigned successively using the standard application of H,H-COSY, HMQC and HMBC experiments. The ^{1}H and ^{13}C chemical shifts of the compounds are presented in Table 1.

On lowering the temperature, the proton signals of the free crown ethers were observed to broaden but

Table 1. ^{1}H and ^{13}C chemical shifts of the maleonitrile tetrathia crown ethers and their complexes with $AgBF_4$

Compound	Chemical shift	**C**N	**C**=**C**	mnS**C**$H_2$$CH_2$S	mnSCH_2**C**H_2S	S**C**$H_2$$CH_2$$CH_2$S	SCH_2**C**$H_2$$CH_2$S
mn–12–S_4	^{13}C	112.8	124.3	38.0	33.8	35.5	
	^{1}H			3.36	2.90	2.95	
[Ag(mn–12–S_4)]BF_4	^{13}C	111.5	124.4	34.1	32.6	32.7	
	^{1}H			3.81	3.30	3.16	
mn–13–S_4	^{13}C	112.6	121.4	35.2	32.0	30.7	31.1
	^{1}H			3.35	3.86	2.66	1.95
[Ag(mn–13–S_4)$_2$]BF_4	^{13}C	113.2	124.5	36.3	34.5	34.8	27.7
	^{1}H			3.77	3.39	3.09	2.21

Table 2. Coalescence temperatures (T_c°C) and and free energies of activation ($\Delta G^{\#}$, kJ mol^{-1}) of the studied compounds

Compound	Parameter	mnS**CH**$_2$CH$_2$S	mnSCH$_2$**CH**$_2$S	S**CH**$_2$CH$_2$CH$_2$S	SCH$_2$**CH**$_2$CH$_2$S
[Ag(mn–12–S$_4$)]BF$_4$	T_c	260	—	246	—
	$\Delta G^{\#}$	66.1	—	65.5	—
[Ag(mn–13–S$_4$)$_2$]BF$_4$	T_c	208	—	—	—
	$\Delta G^{\#}$	52.6	—	—	—

decoalescence did not occur prior to reaching the floor temperature of 176 K. Hence although the ring inversion of the tetrathia crown ethers does slow, it remains too fast to freeze out the preferred conformations spectroscopically. Therefore, the free energies of activation ($\Delta G^{\neq}$) for ring interconversion must be < 20 kJ mol^{-1}.[10] This higher flexibility of maleonitrile crown ethers compared with maleonitrile oxa-thia crown ethers might result from the small C—S—C bond angle which can attain values of $< 90°$ and be due to the long C—S bond.[2]

On lowering the temperature of the Ag(I) complexes of the macrocycles, decoalescence of some of the CH_2 protons was observed. Unfortunately, owing to serious signal overlap, not all of the barriers to ring interconversion could be calculated. The coalescence temperatures (T_c) and $\Delta G^{\neq}$ values that could be observed are listed in Table 2. This increase in the activation barrier to values in excess of 25 kJ mol^{-1} as a result of complex formation is clear evidence for the reduced flexibility of the complexed crowns in comparison with their free states.

Titration experiments

Owing to the rapid interconversion between the free and complexed ligands in solution, only time-averaged values for the chemical shifts of the protons could be observed. Hence, for determination of the ligand-metal stoichiometry, the variations in the chemical shifts of the CH_2 protons were followed whilst titrating the free crown ethers with $AgBF_4$. The observed ^{1}H and ^{13}C chemical shifts of the complexes are also presented in Table 1. During the titration runs, separation of the proton resonances was not observed and therefore the tetrathia crown ethers are still highly flexible even when complexed and can evidently adopt a number of conformations (see below).

To ascertain the stoichiometry of the complexes that were formed, Job's plots were constructed, i.e. plots of $[H_t](\delta_0 - \delta_L)$ versus $[H_t]/([H_t] + [G_t])$. From these plots, the stoichiometry of the reaction is inferred from value of the *x*-coordinate at the plot azimuth. As can be seen from Fig. 2, the maximum for the Ag–mn–12–S$_4$ complex is obtained at $[H_t]/([H_t] + [G_t]) = 0.5$ and for Ag–mn–13–S$_4$ at $[H_t]/([H_t] + [G_t]) = 0.66$. This result means that mn–12–S$_4$ forms 1 : 1 complexes with Ag^+ ions whereas mn–13–S$_4$ formes 2 : 1 complexes with Ag^+. Clearly, then, the ring size of mn–12–S$_4$ is suited for a silver ion to fit into the cavity. Owing to the additional CH_2 group, the increased ring size of mn–13–S$_4$ is too large to position a silver ion into it such that it results in a stable complex. Therefore, a second molecule of mn–13–S$_4$ participates in the complexation. The calculations of the stability constants of these complexes were performed using the method of Rose and Drago[16,17] and the following equation to describe the complex reaction:

$$a[H] + b[G] \rightleftharpoons [C]$$

where [H] is the concentration of the host, [G] that of the guest and [C] that of the complex and a and b are the stoichiometric factors. First, since the concentrations of the ligand (host) and the guest in the equilibrium are unknown, [H] is replaced by $[H_t] - a[C]$ and [G] is replaced by $[G_t] - b[C]$; $[H_t]$ and $[G_t]$ are the known, total concentrations of ligand and metal in solution. Second, the observed chemical shifts (δ_o) are the

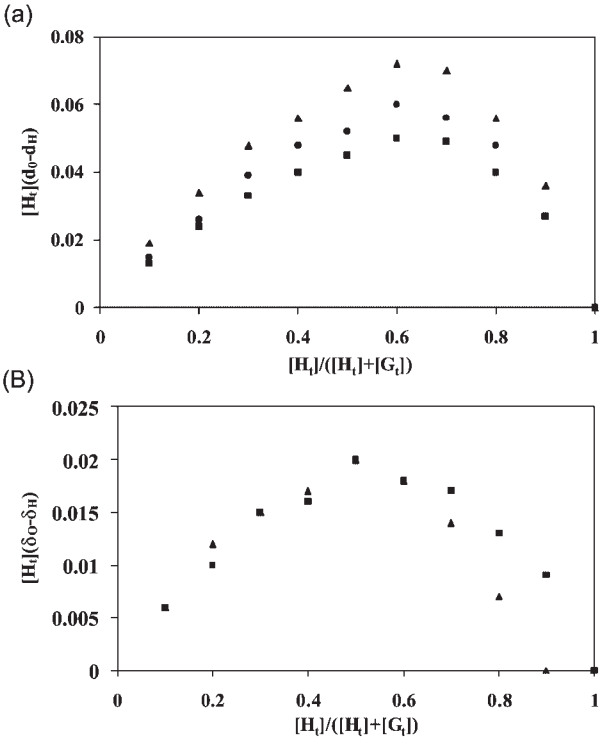

Figure 2. Job's plot for the titrations (A) mn–12–S$_4$ and (B) mn–13–S$_4$ with $AgBF_4$. $[H_t]$, total concentration of the host; $[G_t]$, total concentration of guest; δ_0, observed chemical shift, complex; δ_H, chemical shift, free ligand. ■ mn–S–C**H**$_2$–CH$_2$–S; ▲, mn–S–CH$_2$–C**H**$_2$–S; ●, S–C**H**$_2$–(CH$_2$)–C**H**$_2$–S

weighted averages of the observed chemical shifts of the nuclei of the free (δ_H) and complexed ligand (δ_X), i.e.

$$\delta_o = x\delta_H + (1-x)\delta_C$$

The combination of these two equations enables the calculation of the stability constants for complex formation. The following equation was used in the case of 1:1 complex formation:

$$\frac{1}{K} = ([H_t]\Delta\delta_{max} - [H_t]\Delta\delta)\left(\frac{[G_t]}{[H_t]\Delta\delta} - \frac{1}{\Delta\delta_{max}}\right)$$

and the following equation in the case of 2 : 1 complex formation:

$$\frac{1}{K} = \left(\frac{[H_t]}{\Delta\delta_{max}} - 2[H_t]\Delta\delta\right)^2\left(\frac{[G_t]}{[H_t]\Delta\delta} - \frac{1}{\Delta\delta_{max}}\right)$$

For the complexation of Ag(I) with 1 equiv. of mn–12–S_4:

$$\text{mn–12–}S_4 + AgBF_4 \rightleftharpoons [Ag(\text{mn–12–}S_4)]BF_4$$

a stability constant $\log K = 4.78$ was calculated and for the complexation of Ag(I) with 2 equiv. mn–13–S_4:

$$2\text{mn–13–}S_4 + AgBF_4 \rightleftharpoons [Ag(\text{mn–13–}S_4)_2]BF_4$$

a total stability constant $\log K = 4.66$ was obtained.

Flexibility

To determine the coordinating sites of the crown ethers to Ag(I), the T_1s of the methylene protons of the free ligands and the Ag(I) complexes were measured and are listed in Table 3. The T_1s reflect the inter- and intramolecular mobility, longer T_1 times inferring greater flexibility of a system or part thereof. It is evident from the longer T_1s observed in mn–13–S_4 in comparison with mn–12–S_4 (for corresponding nuclei) that the additional CH_2 group renders greater flexibility to the mn–13–S_4 molecule overall.

Upon complexation, the T_1s of all the methylene protons were found to decrease for both mn–12–S_4 and mn–13–S_4. Therefore, it was concluded that all of the sulfur atoms of the ligands are involved in complexation to the silver cation in both crown ethers despite the differing stoichiometries of the two complexes. For mn–12–S_4, the T_1s of the methylene protons closest linked to the maleonitrile unit (mn–S–C**H**$_2$) were observed to decrease by a proportionately, smaller amount upon complexation in comparison with the T_1s of the other CH_2 groups in the molecule. The inference is that a relatively greater reorientation occurs in the S—CH_2—CH_2—S chain upon complexation and that the CH_2 groups linked closest to the maleonitrile unit are, in fact, predisposed towards complexation.

In mn–13–S_4, on the other hand, the relaxation times of all the CH_2 protons in the molecule decrease equally upon complexation and this decrease was greater than that observed for mn–12–S_4. Owing to the additional CH_2 group, there is greater flexibility in mn–13–S_4 and this extra flexibility is eliminated upon complexation, leading to a greater reduction in the observed T_1s. Based on the T_1s measured for the complexes, the flexibility of the mn–13–S_4 complex was greater than comparison to the mn–12–S_4 complex.

MOLECULAR MODELLING

Flexibility

Since precise information could not be determined from the NMR experiments as regards the conformers of the maleonitrile tetrathia crown ethers in solution (NOEs were not observed and the extracted J couplings adopt values between 6 and 7 Hz, which are average values obtained in rapidly interconverting S—C—C—S fragments), molecular modelling was used to obtain more information concerning the conformational space of the compounds. To examine the intramolecular flexibility of the maleonitrile crown ethers, MD simulations were performed on both crown ethers mn–12–S_4 and mn–13–S_4 and on tetrathia–12–crown–4. The last crown is known to have an *exo*-dentate orientation of its donor atoms[3] and it thus allows a determinate comparison to be made with the two maleonitrile tetrathia crown ethers.

To assess whether the maleonitrile crown ethers have an *endo*- or *exo*-dentate donor arrangement, the distances between neighbouring donor atoms and across the ring were evaluated (see Fig. 3). For [12]ane-S_4, it can readily be seen that the distances between the donor atoms across the ring are longer than the distances between adjacent donor atoms. This is due to the predominant exocyclic arrangement of the donor atoms in [12]ane-S_4.[2] By comparison, for the maleonitrile tetrathia crown ethers,

Table 3. ^{1}H spin–lattice relaxation times T_1 (s) of the maleonitrile tetrathia crown ethers and their complexes with $AgBF_4$

Compound	mnS**C**H$_2$CH$_2$S	mnSCH$_2$**C**H$_2$S	S**C**H$_2$CH$_2$CH$_2$S
mn–12–S_4	0.84	0.82	0.76
[Ag(mn–12–S_4)]BF_4	0.75	0.63	0.57
mn–13–S_4	1.75	1.63	1.94
[Ag(mn–13–S_4)$_2$]BF_4	0.99	1.03	1.00

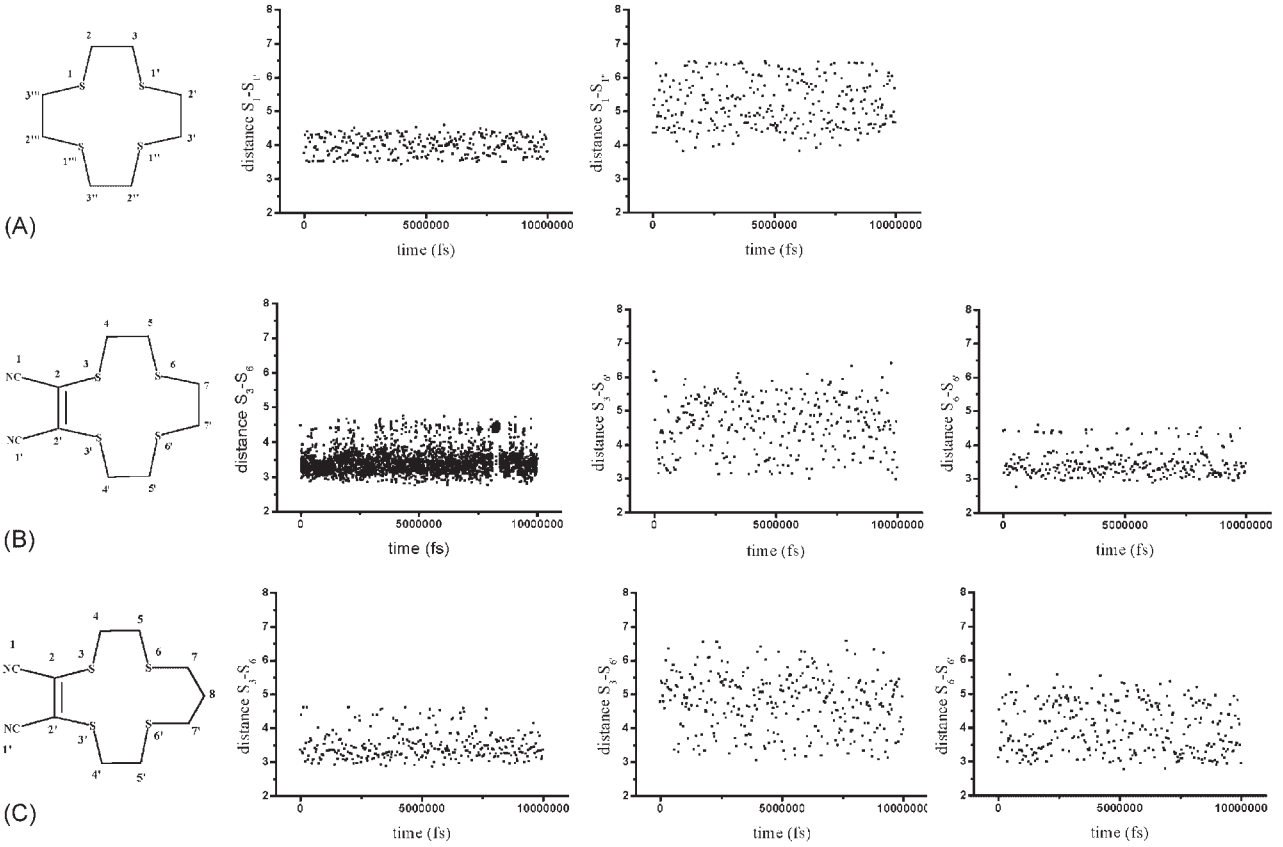

Figure 3. Intramolecular distances in (A) [12]ane-S_4, (B) mn–12–S_4 and (C) mn–13–S_4 plotted against time of the molecular dynamics simulations

the closer distances result from the mainly *endo*-dentate orientation of the sulfur atoms. This preorganization of the donor atoms is one reason for the high stability of the complexes found in the titration experiments.

It can also be seen from Fig. 3 that the distances between the donors across the ring are longer in mn–13–S_4 than in mn–12–S_4. Obviously, the additional CH_2 group in mn–13–S_4 increases the cavity size of the ring and therefore different coordination geometries are adopted by the Ag(I) cation during complexation with each of these crown ethers.

Additionally, it was ascertained from MD simulations that in nearly 80% of the conformations obtained for the two maleonitrile crown ethers, the two equivalent CH_2 groups linked closest to the maleonitrile moiety occupy positions on the same site of the plane of the maleonitrile unit. These conformations are suitable for sandwich or half-sandwich-like complexes whereas the remaining 20% of the conformations with the two equivalent CH_2 groups on opposite sides of the maleonitrile unit plane prefer a tetrahedral coordination sphere (cf. Fig. 4).

Conformational space

Random search simulations were performed to obtain information regarding the preferred conformations of the maleonitrile tetrathia crown ethers in solution. As the result of these searches, several hundred conformations for each crown were obtained, a number too prohibitive to allow individual energy minimizations to be performed. Therefore, and because many of the geometries proved to be very similar to each other, all conformations found by this random search were sorted into groups by application of a family algorithm.[18] Using this technique, distinct families of geometries, where the members of each family reach the same final conformation after geometry optimization, were obtained. For this reason, only one conformation from each family was used for geometry optimization using semiempirical PM3

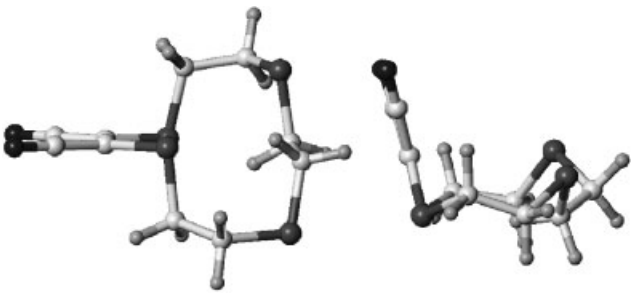

Figure 4. Calculated structures of mn–12–S_4 with the CH_2 groups attached to the maleonitrile unit on different (left) and on the same side (right) of this plane

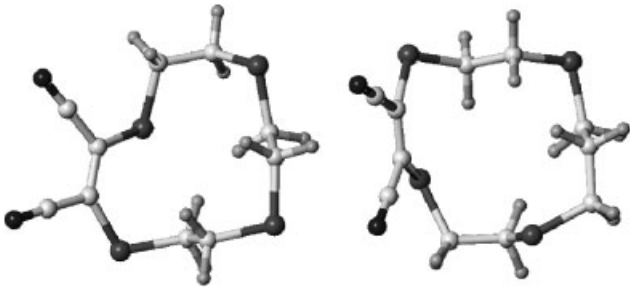

Figure 5. Global minima structures of mn–12–S_4 (left) and mn–13–S_4 (right)

calculations. By this process, 15 conformations were finally found for mn–12–S_4, all of which have energies within 12 kJ mol^{-1} of the global minimum; similarly, 22 final conformations were obtained for mn–13–S_4 (the global minima of mn–12–S_4 and mn–13–S_4 are depicted in Fig. 5). T_1 measurements corroborate this result as they imply much greater flexibility for mn–13–S_4 than mn–12–S_4.

All conformations are characterized by an almost planar maleonitrile unit; the S—C═C—S torsional angle varies between $+4°$ and $-4°$ ($2°$ in the global minimum of mn–12–S_4, $-4°$ in the global minimum of mn–13–S_4). Common to the two maleonitrile crowns is that both the C—S—C—C torsional angles (for the global minimum of mn–12–S_4, $C^2S^3C^4C^5 = 76°$, $C^4C^5S^6C^7 = 84°$, $C^5S^6C^7C^{7'} = -80°$, $C^7C^{7'}S^{6'}C^{5'} = -142°$, $C^{7'}S^{6'}C^{5'}C^{4'} = 84°$, $C^{5'}C^{4'}S^{3'}C^{2'} = 147°$; for the global minimum of mn–13–S_4, $C^2S^3C^4C^5 = -101°$, $C^4C^5S^6C^7 = -154°$, $C^5S^6C^7C^8 = 79°$, $C^8C^{7'}S^{6'}C^{5'} = -58°$, $C^{7'}S^{6'}C^{5'}C^{4'} = -88°$, $C^{5'}C^{4'}S^{3'}C^{2'} = -82°$) and the S—C—C—S torsional angles (for the global minimum of mn–12–S_4, $S^3C^4C^5S^6 = -178°$, $S^6C^7C^{7'}S^{6'} = 168°$, $S^{6'}C^{5'}C^{4'}S^{3'} = -89°$; for the global minimum of mn–13–S_4, $S^3C^4C^5S^6 = 95°$, $S^{6'}C^{5'}C^{4'}S^{3'} = -177°$) prefer synclinal over anticlinal and antiperiplanar dispositions. One notable difference between mn–12–S_4 and mn–13–S_4 is in the C═C—S—C torsional angle. In the smaller 12-membered ring this torsional angle adopts anticlinal or synclinal arrangements (for the global minimum of mn–12–S_4, $C^{2'}C^2S^3C^4 = 46°$, $C^{4'}S^{3'}C^{2'}C^2 = -157°$) whereas in the 13-membered ring this torsional angle adopt antiperiplanar or anticlinal dispositions (for the global minimum of mn–13–S_4, $C^{2'}C^2S^3C^4 = 153°$ and $C^{4'}S^{3'}C^{2'}C^2 = -41°$). The S—C—C—C torsion angles present in mn–13–S_4 also indicate that synclinal over antiperiplanar dispositions are preferred (for the global minimum of mn–13–S_4, $S^6C^7C^8C^{7'} = -91°$ and $C^7C^8C^{7'}S^{6'} = 171°$). The torsion angles for the 10 most stable conformations of mn–12–S_4 and mn–13–S_4 are listed in Tables 4 and 5, respectively. For all of the conformations obtained by PM3 optimization, the two equivalent CH_2 groups linked closest to the maleonitrile unit are positioned on the same side of the plane of the maleonitrile unit.

Table 4. Torsional angles (°) of the 10 most stable conformations of mn–12–S_4 (for numbering of the atoms, see Fig. 3)

Conformation	2′–2–3–4	2–3–4–5	3–4–5–6	4–5–6–7	5–6–7–7′	6–7–7′–6′	7–7′–6′–5′	7′–6′–5′–4′	6′–5′–4′–3′	5′–4′–3′–2′	4′–3′–2′–2	3′–2′–2–3	E (kJ mol^{-1})
1	46	76	−178	84	−80	168	−142	84	−89	147	−157	2	0.0
2	145	108	95	−99	112	175	73	82	−105	97	−135	0	1.7
3	140	−106	76	−129	71	115	−92	−86	76	70	−138	0	2.3
4	152	−100	94	−139	47	84	−165	76	84	−90	−42	−2	2.8
5	54	−109	176	−81	−81	166	−103	83	−98	179	−153	3	4.4
6	49	−108	−179	−82	−83	165	−88	68	−119	−166	−29	1	4.4
7	150	−101	111	−85	−56	163	−133	67	73	−95	−42	−3	4.7
8	138	−108	78	−96	180	−102	−68	122	−80	104	−149	2	4.8
9	149	−104	80	−122	68	102	180	96	−78	108	−138	0	4.8
10	156	−141	89	−88	146	−93	−74	82	94	−82	−46	−1	5.1

Table 5. Torsion angles of the 10 most stable conformations of mn–13–S_4 (for numbering of the atoms, see Fig. 3)

Conformation	2′–2–3–4	2–3–4–5	3–4–5–6	4–5–6–7	5–6–7–8	6–7–8–7′	7–8–7′–6′	8–7′–6′–5′	7′–6′–5′–4′	6′–5′–4′–3′	5′–4′–3′–2′	4′–3′–2′–2	3′–2′–2–3	E (kJ mol^{-1})
1	153	−101	95	−154	79	−91	171	−58	−88	−177	−82	−41	−4	0.0
2	172	−75	−79	103	−98	177	−80	−87	71	105	−91	−48	0	4.3
3	−152	71	74	−118	85	−178	177	−85	118	−75	−72	152	0	4.9
4	−147	71	77	−126	40	179	175	73	−123	89	−106	150	0	5.8
5	−142	98	−96	147	−100	87	171	76	92	−72	−70	150	2	5.8
6	−149	136	−90	96	−114	164	173	65	74	−86	−68	146	1	6.6
7	53	78	179	89	−104	176	−83	−59	151	−107	117	−157	4	6.7
8	−49	−90	94	55	−158	178	−72	−49	141	−77	−79	169	−1	6.9
9	−169	78	76	−142	48	71	−179	157	−56	−95	89	49	1	6.9
10	−144	119	−82	122	−96	−77	−172	−94	103	−80	−68	154	3	7.0

Conformations of the Ag(I) complexes

All of the low-energy conformations which had been obtained by random search simulation followed by PM3 optimization were then studied with respect to the conformational space of their Ag(I) complexes. Since the titration experiments provided the stoichiometries of the complexes and from the T_1s it was evident that all four sulfur atoms were participating in complex formation in both complexes, an Ag^+ ion was centred in the middle of one mn–12–S_4 ring for the complexes of mn–12–S_4, and between two mn–13–S_4 molecules for the complexes of mn–13–S_4. The structures were then optimized semiempirically using ZINDO calculations.[15] Owing to complexation to the Ag^+ ions, the maleonitrile tetrathia crown ethers experience reduced flexibility, as was indicated by the reduced T_1s of the methylene protons and only a total of four conformers for $[Ag(mn–12–S_4)]^+$ and a total of seven conformers for $[Ag(mn–13–S_4)_2]^+$ were obtained; the non-global mimina all had energies within 12 kJ mol^{-1} of the respective global minima of the two complexes (see Fig. 6 for these global minima).

From the result of these calculations, it was deduced that the Ag(I) cation fits neatly into the mn–12–S_4 ring and that it forms a tetrahedral complex. This is not possible in the case of mn–13–S_4 owing to the larger ring size of the 13-membered ring (see above). The additional CH_2 group enlarges the size of the ring so that not all four donor atoms can participate in the coordination of the silver(I) center without building up additional conformational strain. Moreover, the altered conformational flexibility now allows the four donor atoms to point to one side of the thiocrown ether unit. Therefore, the Ag^+ cation forms a 2 : 1 sandwich complex with mn–13–S_4. This theoretical result readily explains the different geometries of the Ag(I) complexes of mn–12–S_4 and mn–13–S_4. First, in $[Ag(mn–12–S_4)]^+$ the two equivalent CH_2 groups linked closest to the maleonitrile unit occupy positions on different sides of the maleonitrile plane. By contrast, in $[Ag(mn–13–S_4)_2]^+$ these CH_2 groups are located on the same side of this plane so that the sandwich complex can be realized.

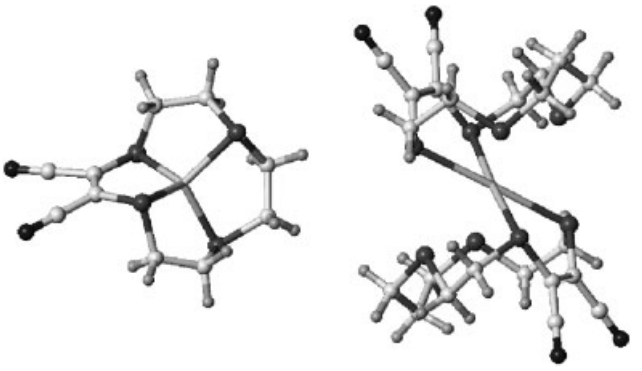

Figure 6. Global minima structures of $[Ag(mn–12–S_4)]^+$ and $[Ag(mn–13–S_4)]^+$

Table 6. Torsion angles of the four most stable conformations of $[Ag(mn\text{–}12\text{–}S_4)]^+$ (for numbering of the atoms, see Fig. 3)

Conformation	2′–2–3–4	2–3–4–5	3–4–5–6	4–5–6–7	5–6–7–7′	6–7–7′–6′	7–7′–6′–5′	7′–6′–5′–4′	6′–5′–4′–3′	5′–4′–3′–2′	4′–3′–2′–2	3′–2′–2–3	E (kJ mol^{-1})
1	53	−129	97	−124	48	50	47	−114	23	−70	116	−18	0.0
2	−111	69	−39	133	−88	29	−105	58	82	−105	93	−20	2.9
3	−105	31	53	57	−133	70	−113	63	79	−110	84	−15	5.0
4	−84	155	−98	134	−71	30	−106	104	−91	132	−61	3	9.0

Table 7. Torsion angles of the seven most stable conformations of $[Ag(mn\text{–}13\text{–}S_4)_2]^+$ (for numbering of the atoms, see Fig. 3)

Conformation	2′–2–3–4	2–3–4–5	3–4–5–6	4–5–6–7	5–6–7–8	6–7–8–7′	7–8–7′–6′	8–7′–6′–5′	7′–6′–5′–4′	6′–5′–4′–3′	5′–4′–3′–2′	4′–3′–2′–2	3′–2′–2–3	E (kJ mol^{-1})
1	−162	74	41	180	101	75	−82	−68	−172	−57	−75	132	16	0.0
	−154	74	48	−176	89	78	−84	−74	−161	−105	−176	−70	6	
2	−143	48	69	−168	65	100	−48	−111	32	102	−124	124	0	2.0
	−128	45	74	−161	56	104	−52	116	−84	57	−167	155	−10	
3	−127	107	−48	−60	−169	−83	79	−174	50	52	−109	158	−20	8.0
	−136	87	−24	−66	−152	−35	−43	−66	78	65	−136	139	−1	
4	−70	−141	−103	69	57	171	−90	−66	−174	−73	−65	151	−19	9.0
	−147	36	57	155	106	84	−82	−62	−178	−76	−50	139	4	
5	−135	33	34	122	−170	−25	79	−141	175	−69	−53	146	1	11.0
	−139	33	29	128	−179	−21	82	−150	169	−69	−48	145	2	
6	−119	145	−71	−67	108	77	−82	−101	62	69	−145	133	−6	12.0
	−110	155	−71	−77	88	90	−71	−111	64	74	−154	125	−7	
7	−154	60	−17	152	−155	−31	82	−138	172	−66	−49	148	5	12.0
	−153	57	−12	149	−96	84	115	−173	172	−66	−49	149	5	

Second, different preferences are also observed for the torsion angles in the two complexes. Whereas in $[Ag(mn–12–S_4)]^+$ synclinal or anticlinal conformations for the C═C—S—C and C—C—S—C fragments were found, the corresponding torsion angles in $[Ag(mn–13–S_4)_2]^+$ were characteristic for antiperiplanar conformations. The S—C—C—S torsion angles in both complexes and also the S—C—C—C torsion angles in $[Ag(mn–13–S_4)_2]^+$ indicate the preference for synclinal over anticlinal conformations. The torsion angles for the four most stable conformations of $[Ag(mn–12–S_4)]^+$ and the seven most stable conformations $[Ag(mn–13–S_4)_2]^+$ are listed in Tables 6 and 7, respectively.

Third, the distances of the donor atoms across the macrocyclic ring system range from 3.65 to 3.87 Å in $[Ag(mn–12–S_4)]^+$, but from 4.33 to 5.15 Å in $[Ag(mn–13–S_4)_2]^+$. These distances differ only slightly from the corresponding values in the free ligands. This is also a good indication of the preorganization of the donor atoms in the free ligands towards the complexation of Ag(I) ions. Finally, the calculated Ag^+—S distances vary between 2.52 and 2.60 Å in $[Ag(mn–12–S_4)]^+$ and between 2.65 and 2.83 Å in $[Ag(mn–13–S_4)_2]^+$. This theoretical result is in good agreement with Ag^+—S distances known from crystal structures of similar crowns, which were found to vary between 2.40 and 2.92 Å, depending on the coordination geometry.[19] The shorter Ag^+—S distance in $[Ag(mn–12–S_4)]^+$ in comparison with the Ag^+—S distance in $[Ag(mn–13–S_4)_2]^+$ may in part explain the slightly higher stability constant of the former complex.

CONCLUSIONS

The preferred conformers of the novel maleonitrile tetrathia crown ethers mn–12–S_4 and mn–13–S_4 and of their complexes with $AgBF_4$ in solution were studied by both NMR spectroscopy and molecular modelling. The tetrathia crown ethers were found to be highly flexible but with a preorganized endocyclic arrangement of donor atoms.

Mainly owing to the ring size, mn–12–S_4 forms 1:1 complexes with Ag(I) ions whereas mn–13–S_4 forms 2 : 1 complexes in solution. In the so-formed complexes, Ag(I) coordinates to all four donor atoms of the macrocyclic rings in both cases, thereby effecting a reduction in the intramolecular flexibility for both systems. Different solution geometries for the Ag(I) complexes were also obtained: tetrahedral coordination to Ag(I) for one mn–12–S_4 molecule but sandwich-like coordination of two mn–13–S_4 crown ether molecules to one Ag(I) cation.

REFERENCES

1. (a) Lange SJ, Sibert JW, Stern CL, Barrett AGM, Hoffman BM. *Tetrahedron* 1995; **51**: 8175–8188; (b) Holdt H-J, Poetter M. *Inorg. Chim. Acta* to be published.
2. Wolf RE. *J. Am. Chem. Soc.* 1987; **109**: 4328–4338.
3. (a) Hiraoka M. *Studies in Organic Chemistry 12: Crown Compounds*. Elsevier: Amsterdam, 1982; (b) Inoue Y, Gokel GW (eds). *Cation Binding by Macrocycles*. Marcel Dekker: New York, 1990; (c) Lehn JM, Atwood JL, Davies JED, MacNicol DD, Vögtle F (series eds). *Comprehensive Supramolecular Chemistry*, vols 1–11. Pergamon/ Elsevier: Oxford, 1996.
4. Kleinpeter E, Grotjahn M, Klika KD, Drexler H-J, Holdt H-J. *J. Chem. Soc., Perkin Trans. 2* 2001; 988–993.
5. Grotjahn M, Drexler H-J, Jäger N, Holdt H-J, Kleinpeter E. *J. Mol. Model.* 1997; **3**: 355–358.
6. (a) Drexler H-J, Reinke H, Holdt H-J. *Chem. Ber.* 1996; **129**: 807–820; (b) Drexler H-J, Grotjahn M, Holdt H-J, Kleinpeter E. *Inorg.Chim. Acta* 1999; **285**: 305–308; (c) Drexler H-J, Starke I, Grotjahn M, Reinke H, Holdt H-J, Kleinpeter E. *Z. Naturforsch*., 1999; **546**: 799–806.
7. Drexler H-J, Starke I, Grotjahn M, Holdt H-J, Kleinpeter E. *Inorg. Chim. Acta* 2001; **317**: 133–142.
8. Grotjahn M, Jäger N, Drexler H-J, Holdt H-J, Kleinpeter E. *J. Mol. Model*. 1999; **5**: 72–77.
9. Gutowski HS, Holm CH. *J. Chem. Phys.* 1956; **25**: 1228–1234.
10. Friebolin H. *Ein- und Zweidimensionale NMR-Spektroskopie*. VCH: Weinheim, 1988.
11. (a) Shibata Y, Inoue B, Nakatuka Y. *Nippon Kagaku Kaishi* 1921; **42**: 983–1005; (b) Tsuchida R. *Bull. Chem. Soc. Jpn.* 1935; **10**: 27–39; (c) Job P. *C. R. Acad. Sci.* 1925; **180**: 928–930; (d) Job P. *Ann. Chim. Phys.* 1928; **9**: 113–203.
12. *SYBYL Molecular Modelling Software, Version 6.8*. Tripos: St. Louis, MO, 2001.
13. Clark M, Cramer RD III, van Opdenbosch N. *J. Comput. Chem*. 1989; **10**: 982–1012.
14. *SYBYL Molecular Modelling Software, Force Field Manual Version 6.8*. Tripos: St. Louis, MO, 2001.
15. (a) Zerner M, Loew GH, Kirchner RF, Mueller-Westerhoff UT. *J. Am. Chem. Soc*. 1980; **102**: 589–599; (b) Anderson WP, Edwards WD, Zerner MC. *Inorg. Chem*. 1986; **25**: 2728–2732; (c) Zerner MC. *Reviews in Computational Chemistry II*. VCH: New York, 1991; Chap. 8, 313–365; (d) Bacon AD, Zerner MC. *Theor. Chim. Acta* 1979; **53**: 21–54; (e) Anderson WP, Cundari TR, Zerner MC. *Int. J. Quantum Chem.* 1991; **39**: 31–45.
16. (a) Rose NJ, Drago RS, *J. Am. Chem. Soc*. 1959; **81**: 6138–6141; (b) Nagakura S, Nakano NI, Higuchi T. *J. Am. Chem. Soc*. 1958; **80**: 520–524.
17. Hirose K. *J. Inclusion Phenom.* 2001; **39**: 193–209.
18. *SYBYL Molecular Modelling Software, Molecular Spreadsheet Manual, Version 6.8*. Tripos: St. Louis, MO, 2001.
19. *CSD Cambridge Structural Database*. Crystallographic Data Centre: Cambridge.